Journal of Engineering and Technology for Industrial Applications

ITEGAM-JETIA

Manaus, v.10 n.47, p. 159-171. May/June., 2024.
DOI: https://doi.org/10.5935/jetia.v10i47.1166

ISSN ONLINE: 2447-0228

RESEARCH ARTICLE OPEN ACCESS

DIGITAL TWIN OF A PHOTOVOLTAIC SYSTEM

Luis Gabriel Fong Mollineda[1] and José Rafael Abreu García[2]

[1,2] Central University "Marta Abreu" of Las Villas – Santa Clara, Cuba.

[1] http://orcid.org/0009-0003-7581-3276 , [2] http://orcid.org/0000-0002-8344-8796

Email: [1]lfomg@uclv.cu,[2] abreu@uclv.edu.cu

ARTICLE INFO

Article History
Received: June 26th, 2024
Revised: June 026th, 2024
Accepted: June 27th, 2024
Published: July 01th, 2024

Keywords:
Digital Twin,
Matlab,
Simulink,
Raspberry Pi.

ABSTRACT

The creation of a Digital Twin, for the simulation of the photovoltaic park installed at the UCLV, which establishes a bidirectional data exchange in real time with the aim of providing a precise virtual copy, in order to monitor it and analyze its reaction to certain stimuli. or circumstances to improve its performance and extend its useful life. A virtual model is built using two tools: Simulink, and the PV_LIB Toolbox in Matlab. The implementation is carried out on a Raspberry Pi model B+. The connection between Matlab and the Raspberry Pi is achieved using appropriate support packages, allowing the Digital Twin to run constantly. The input data comes from the UCLV photovoltaic park, obtained through the ThingSpeak platform, while the outputs include current, voltage and power. The main focus of this work is to achieve the connection between Matlab and the Raspberry Pi, find a virtual model that fits the real plant, its implementation in code and validate the power generation of the Digital Twin in relation to the Physical Twin through root mean square error (RMSE).

I. INTRODUCTION

Various works have been carried out at the UCLV that are based on the modeling of photovoltaic systems and their control, however, the models obtained do not involve all the factors that influence their behavior and do not allow the exchange of information with the system. A step forward in working with complex systems, such as photovoltaics, is the use of a Digital Twin.

The use of a digital twin allows to simulate the behavior of the photovoltaic system in different conditions and scenarios, this makes it possible to optimize the system design and maximize its performance. It can also help identify and correct problems in the design or operation of the system before its implementation, reducing the costs associated with repairs and maintenance. Energy efficiency increases identifying the weak points of the system. It can be used to monitor the photovoltaic system in real time and detect possible failures or early anticipate problems, reducing inactivity time and facilitating its maintenance [1]. Obtaining clean and safe energy for the environment reduces the need to use polluting energy sources, thus reducing the emission of greenhouse gases and contributing to the fight against climate change [2].

Digital twin technology is relatively new, but its origin dates back to the second half of the last century, in the aeronautical industry, with the idea of creating a real-time virtual representation of physical systems. Over time, it has expanded to other industries such as energy, automotive, and manufacturing, among others. Today, digital twins are a valuable tool for the simulation and monitoring of complex physical systems in different fields [3].

Regarding the photovoltaic industry, the use of digital twins is a field in constant evolution. In recent years, there has been an increase in research and development of digital twins focused on solar energy, with the aim of improving the performance and efficiency of photovoltaic systems [4].

To establish a Digital Twin of a photovoltaic system, a digital representation of the system is needed that includes: information about the components, geometry, climate and other factors that affect the performance of the system, this being the physical model; The mathematical equations that describe the behavior of the components of the photovoltaic system: solar

panels, inverter and others, constitute the mathematical model. Implementation of software that uses physical and mathematical models to simulate the behavior of the photovoltaic system in different conditions and scenarios, having the data analysis tool to identify patterns, trends and anomalies in real-time monitoring data on the climate, solar radiation, temperature and other affecting factors. The user interface allows you to interact with the Digital Twin, view the data and results of the simulation [5].

This article proposes to create a Digital Twin of the UCLV photovoltaic park. To achieve this, it is necessary to characterize the installed photovoltaic park, determine the fundamental parameters necessary to form a Digital Twin, analyze the characteristics of the main software to be used in digital twins and select the most suitable for the application

II. STATE OF THE ART OF DIGITAL TWINS IN PHOTOVOLTAIC SYSTEMS.

II.1 DIGITAL TWIN.

A Digital Twin is a digital representation of a physical object or system, which establishes a bidirectional data exchange in real time. The objective of a Digital Twin is to provide an accurate and detailed virtual copy of a physical element, in order to monitor it and analyze its reaction to certain stimuli or circumstances [6],[7].

It must be clear that the Digital Twin is not a new idea since its concept originated during the penultimate decade of the last century, dating back to the APOLO program of the National Aeronautics and Space Administration (NASA). In this program, two identical space vehicles were built in order to simulate the behavior of their ships, equipment and the physical integrity of the crew members. During the mission to space, the terrestrial acted as a twin and was used to reflect flight conditions using available flight data [6].

The Digital Twin has constantly evolved over the years and is expected to continue evolving in the next decade. Currently, it has become an essential component for the digital transformation of the industry. This technology is used in 34% of companies globally, and with improvements of more than 25% in system performance. Its implementation has shown a 15% increase in key sales and operational metrics with an average of 16% in sustainability, driving implementation by 36% over the next five years; This is revealed by the report "Digital Twins: Adding Intelligence to the Real World" from the Capgemini Research Institute (Spain) in 2022 [8].

Implementation can be complex, given the wide range of functionalities it must support. It is built so that it can receive information from sensors to measure real-time parameters of physical elements, interacting with virtual space through the industrial internet of things [9].

II.2 DIGITAL TWINS IN THE PHOTOVOLTAIC INDUSTRY.

In the photovoltaic industry, digital twins are used to represent photovoltaic systems, from individual solar panels to entire solar parks. They allow photovoltaic system engineers and operators to simulate different operating scenarios and evaluate their impact on system performance. For example, different weather conditions, variations in the inclination and orientation of the solar panels, and changes in the electrical load of the system can be simulated. In addition, they can help predict and prevent possible failures or problems in the photovoltaic system [10].

In recent years, research has been conducted on the use of digital twins to improve the efficiency and performance of photovoltaic systems, especially in terms of power production prediction, fault detection and predictive maintenance.

Figure 1 presents the architecture of a Digital Twin in the photovoltaic industry, in which several blocks that work together to create a virtual replica of the system can be identified [11]:

• Digital shadow: digital footprint left by the Digital Twin and is made up of a database and interfaces, the latter being responsible for interacting with the database and implementing machine learning methods; since it is necessary for data prediction and to restore the system's behavioral model.

• Digital model: is responsible for the operation of the entire system by implementing the interface of interactions with the other components of the digital model, such as a mathematical model and a system for collecting operational information.

• Control system: introduces a control action on a real object, whose prototype is a Digital Twin.

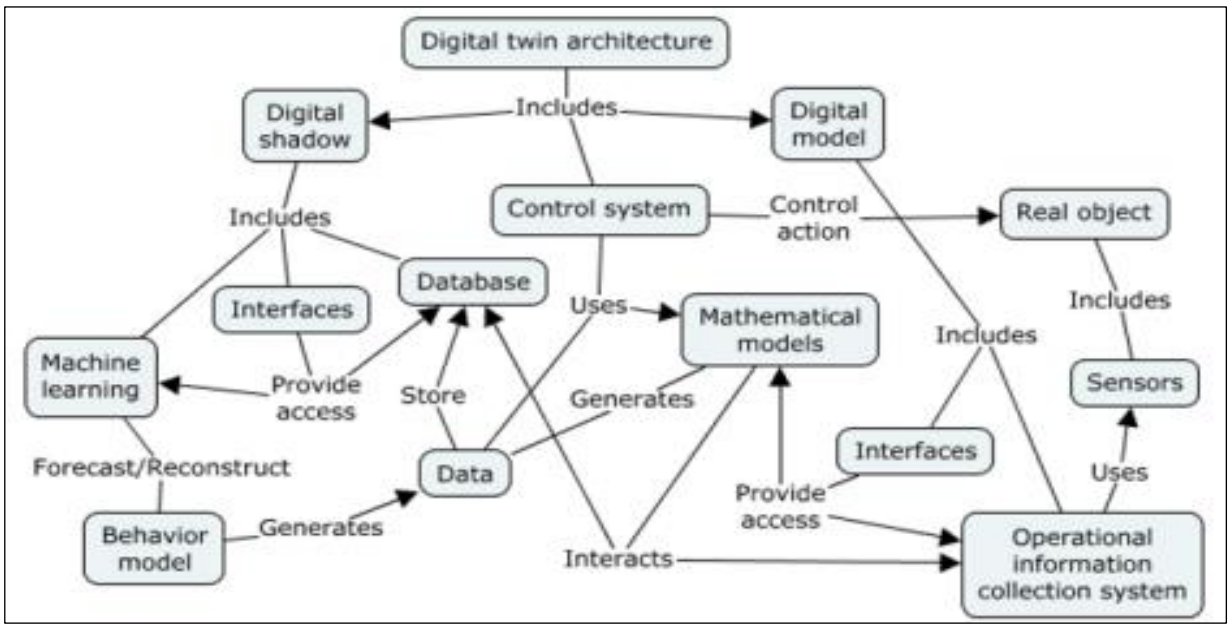

Figure 1: Digital twin architecture.

Source: Authors, (2024).

III. FUNDAMENTAL ASPECTS OF PHOTOVOLTAIC FIELDS EXEMPLIFYING THE ONE INSTALLED AT UCLV.

III.1 CELL, PANEL AND PHOTOVOLTAIC SYSTEM.

The solar cell is the central component of photovoltaic solar panels, playing a fundamental role in converting solar radiation into electrical energy through the photovoltaic effect. In its composition, a semiconductor material is mainly used, silicon being the most commonly used. Depending on the desired level of efficiency, monocrystalline or polycrystalline silicon can be used. Monocrystalline silicon is considered one of the most efficient materials for manufacturing solar cells, due to its ability to achieve high efficiency in converting sunlight into electricity [12],[13].

In 1905, Einstein proposed the model of the photoelectric effect, where he assumed that the light energy was not distributed uniformly throughout the expanding wave front, but in separate packets. The energy of light, in the form of a beam that has a certain frequency, is presented in discrete packets called photons. Each photon carries with it an amount of energy represented by the formula E = h*f ≥ Eg (Forbidden Energy Band), where h is Planck's constant (h = 6.626·10-34 J·s) and f is the frequency of the light beam. In this way, for the effect to occur, the energy of the photon must be greater than the energy of the electron for it to be expelled from the material [14].

There are two fundamental parameters that define the electrical properties of a photovoltaic solar cell: the open circuit voltage and the short circuit current. The open circuit voltage (Voc) refers to the difference in electrical potential that occurs at the terminals of the cell when there is no load connected, which means that the current is zero. On the other hand, the short circuit current (Isc) is the maximum value reached by the current at a given instant when the cell is directly connected without resistance, that is, when the voltage is equal to zero. These parameters are of vital importance to understand the behavior and efficiency of a solar cell [15].

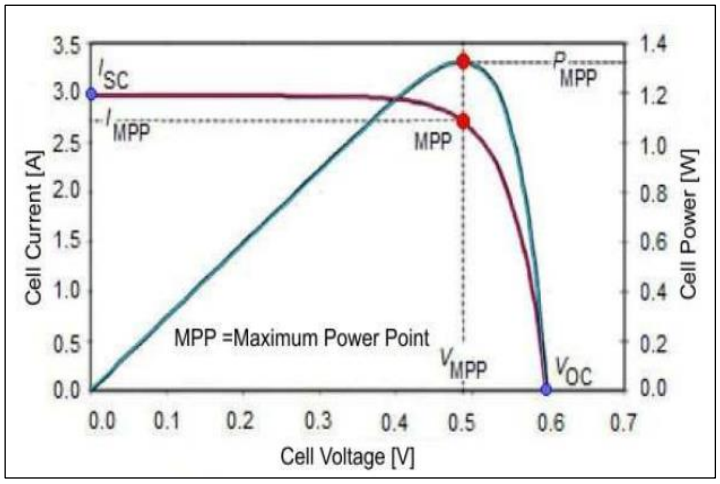

Figure 2: Characteristic curves of a photovoltaic solar cell.
Source: Authors, (2024).

The representation of a solar cell is made through a model that uses a simplified circuit composed of a classic p-n junction diode, and electronic components such as sources and resistive elements that emulate the losses represented in a real environment.

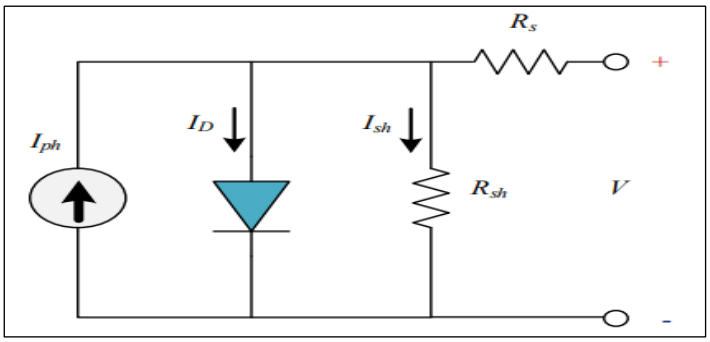

Figure 3: Equivalent circuit of a solar panel.
Source: Authors, (2024).

The simple diode model proposed by Gow 1999 demonstrates the relationship between current and voltage delivered by a photovoltaic module. By applying Kirchhoff's law to the circuit in Figure 3, the current generated (Icel) by the solar panel can be deduced:

$$\text{Icel} = \text{Iph} - \text{Id} - \text{Ish} \quad (1)$$

$$\text{cel} = \text{Iph} - \text{Io}[e^{\frac{q(V+\text{Icel}*Rs)}{KTcA}} - 1] - \frac{V + \text{Icel} * R}{Rsh} \quad (2)$$

Where Iph is the photogenerated current, Io is the reverse saturation current of the diode, q is the electron charge (1.6 x 10-19 C), V solar cell voltage, K is the Boltzmann constant (1, 38 x 10-23 J/K), Tc cell operating temperature and A ideality factor. The currents exhibit an almost linear relationship with respect to radiation (Iph) and temperature (Tc).

The current generated by a solar cell is affected by the intensity of solar radiation and the temperature of the cell at the time of measurement. These two factors influence the amount of photogenerated current, as stated in equation 3.

$$\text{Iph} = \frac{R}{Rref}[\text{Ilref} + \text{UIsc}(\text{Tc} - \text{Tcref})] \quad (3)$$

Considering the following parameters: R represents the solar radiation measured at the current moment, Rref is the solar radiation under standard conditions of 1000 W/m2, Ilref is the photogenerated current under reference conditions, which is taken as the short circuit current (Isc =Ilref), UIsc is the temperature coefficient of the short circuit current, and Tcref is the working temperature of the cell under standard conditions (298°K). Furthermore, the reverse saturation current of the diode also depends on temperature, and this is described by equation 4:

$$\text{Io} = \text{Ioref}\left(\frac{\text{Tc}}{\text{Tcref}}\right)^3 * e^{\left[\frac{qEg\left(\frac{1}{Tref} - \frac{1}{Tc}\right)}{KA}\right]} \quad (4)$$

In relation to this, Ioref represents the reverse saturation current under reference conditions, while Eg corresponds to the energy of the semiconductor in its bandgap. The current Ioref is defined according to equation 5.

$$\text{Ioref} = \frac{\text{Isc}}{e^{\left(\frac{\text{Voc}}{Ns*K*Tc*A}\right)} - 1} \quad (5)$$

Typically, solar cells have an output of around 2W at 5V [16], which requires them to be grouped in series or parallel configurations to achieve the desired power. To do this, the coefficients Np, which denotes the number of modules in parallel, and Ns, which represents the number of cells in series, are added to the current-voltage characteristic equation of a photovoltaic cell described in 2. Equation 6 describes the current-voltage relationship of a solar panel.

$$\text{Ipanel} = \text{Np} * \text{Iph} - \text{Np} * \text{Io} \left[e^{\frac{q\left(\frac{V}{Ns}+\frac{Icel*Rs}{Np}\right)}{K*Tc*A}} - 1 \right] - \frac{V\left(\frac{Np}{Ns}\right) + Icel * Rs}{Rsh} \quad (6)$$

Equation 6 is generally reduced to 7, since authors such as Granda-Gutiérrez [17], Huan-Liang Tsai [16], De Soto, Klein, and Beckman [18], Xuan Hieu Nguyen and Minh Puhong Nguyen [19], simplify the equation because the shunt resistance does not affect the efficiency of a solar cell, because the resistance tends to be very large or infinite, so we can assume Rsh=∞. But the series resistance does significantly affect the behavior of the cell, therefore [20], [21]:

$$\text{Ipanel} = \text{Np} * \text{Iph} - \text{Np} * \text{Io} \left[e^{\frac{q\left(\frac{V}{Ns}+\frac{Icel*Rs}{Np}\right)}{K*Tc*A}} - 1 \right] \quad (7)$$

Photovoltaic modules are born from a mosaic of solar cells. A solar panel is a broader term used to describe a complete system that includes multiple interconnected photovoltaic modules, along with other components necessary for its operation, such as cables, connectors, inverters, and mounting structures. It is responsible for converting solar radiation into electrical energy, transforming it into direct current. These panels are composed of multiple configurations of solar cells connected in series and/or in parallel to achieve the desired voltage and current conditions. First, the desired voltage is established by grouping the solar cells in series. Once the voltage is determined, the branches with the solar cells in series are grouped in parallel to achieve the necessary current. Therefore, the specific power is achieved through the combination of the number of solar cells and the type of connection between them [22].

Elements of a photovoltaic panel [23]:

• Solar cells: These are the fundamental components that convert sunlight into electricity.

• Frame: It is the structure that surrounds and protects the solar cells.

• Front glass: It is a transparent layer of glass that covers the solar cells. It protects cells from mechanical damage, such as impacts, dust and moisture, while allowing sunlight to pass through.

• Encapsulating: It is a resistant and transparent material, generally a polymer sheet such as EVA (ethylene-vinyl acetate), which is placed between the solar cells and the front glass.

• Electrical connections: Photovoltaic panels have electrical connections that allow the transfer of current generated by the solar cells.

• Junction Box: This is a sealed box located on the back of the panel that houses the electrical connections and protects the cables and connections from damage and adverse environmental conditions.

There are two main categories of photovoltaic systems: stand-alone systems and grid-connected systems. The key distinction between these two systems lies in their ability to manage excess energy. In a stand-alone photovoltaic system, it is necessary to have a regulator that manages the storage of additional energy generated during sunlight hours in batteries. This allows this stored energy to be used at times when solar production is not enough. On the other hand, a system connected to the electrical grid has the advantage of taking advantage of the support of the grid to supply energy in times of generation deficiency and also to inject excess generated energy. The energy exchange is recorded through a meter that measures both the amount of energy demanded from the electrical grid when solar production is insufficient, and the amount of energy delivered to the grid when there is a surplus of energy generated [24].

III.2 SOFTWARE AND PHYSICAL DEVICE ENVIRONMENTS USED.

Software environments used

The advancement of the Digital Twin has been made using two different approaches: Simulink and PV_LIB. The reason for using both tools is that Simulink does not allow modeling the impact of temperature, while PV_LIB cannot be implemented on the hardware board. In addition to these Matlab tools, the help of other utilities has also been required such as ThingSpeak to obtain the input data from the cloud, and VNC Viewer to establish a remote connection between the computer and the Raspberry Pi.

Matlab: is a programming and numerical computing platform that has an integrated development environment and its own programming language based on matrices, the M language. Its features include data analysis, representation of data and functions using graphs, development and implementation of algorithms, creation of web and desktop applications, ability to use Matlab with other languages, cloud computing and connection between Matlab and other hardware equipment [25].

Simulink: is a visual programming environment based on block diagrams from the Matlab programming environment. This tool is used to design systems based on multi-domain models, design and simulate before hardware implementation and deploy without having to write code [26].

PV_LIB Toolbox – Provides a set of well-documented functions to simulate the performance of photovoltaic power systems. It allows calculating irradiation and solar position, decomposition of irradiance and transposition to the plane of the matrix, dirt and shading, cell temperature, obtaining power through irradiance, losses due to mismatch in resistance and due to electrical mismatch of direct current, maximum power point tracking, inverter efficiency, alternating current losses and long-term degradation [27].

ThingSpeak: is an Internet of Things (IoT) analytics platform created in 2010 by ioBridge. Its primary goal is to provide support for IoT applications by enabling real-time data collection, visualization, and analysis in the cloud. Facilitates the sending of data from devices connected to the internet. Then, you can analyze and visualize that data using the Matlab tool [28].

VNCviewer: is a free source software based on a client-server structure, in which the client computer can view the screen and control and interact with the server computer's equipment remotely. It does not take into account the operating system of the server computer with respect to the client computer, any operating system that supports VNC is needed to establish communication. This software was created in the United Kingdom, specifically at "AT&T Olivetti Research Laboratory" based on the RFB (Remote Frame Buffer) protocol [29].

Raspberry Pi

The Raspberry Pi is an inexpensive, low-power, compact-sized computing device. Its main objective is not to have an extremely powerful processor, but to be a small computer capable of operating 24 hours a day with minimal energy consumption.

This small board computer requires additional components to function correctly. It is necessary to use a microSD card to load the Raspberry Pi operating system (in this case, a 16 GB microSD card is used). The official operating system is the Raspberry Pi OS, which is a version of Debian, although it is also compatible with other operating systems such as Windows 10. Additionally, an external power supply is required for the Raspberry Pi, which must provide at least 2 amps. of current [30].

Raspberry Pi model B+

The Raspberry Pi model B+ figure 4, was released by the Raspberry Pi Foundation in July 2014 as an upgrade to the original Raspberry Pi model B. It has the following characteristics [31]:

1. Processor: Uses a 32-bit Broadcom BCM2835 processor, with an ARMv6 core running at 700 MHz.
2. Memory: it has 512 MB of RAM.
3. Connectivity: It has four USB 2.0 ports, an Ethernet port (RJ-45), an HDMI output, a composite video output, a microSD card slot, a 3.5 mm audio jack and a CSI camera connector.
4. Storage: Use a microSD card as the main storage medium.
5. GPIO: It has 40 GPIO pins that allow the connection of additional electronic components.
6. Power: Powered through a 1.8 A – 5V microUSB connector.
7. Size: It has a compact form factor, with dimensions of approximately 85 x 56 x 17 mm.

It's important to note that the Raspberry Pi Model B+ has been replaced by newer models, such as the Raspberry Pi 3 Model B+ and Raspberry Pi 4 Model B, which offer better performance and additional features.

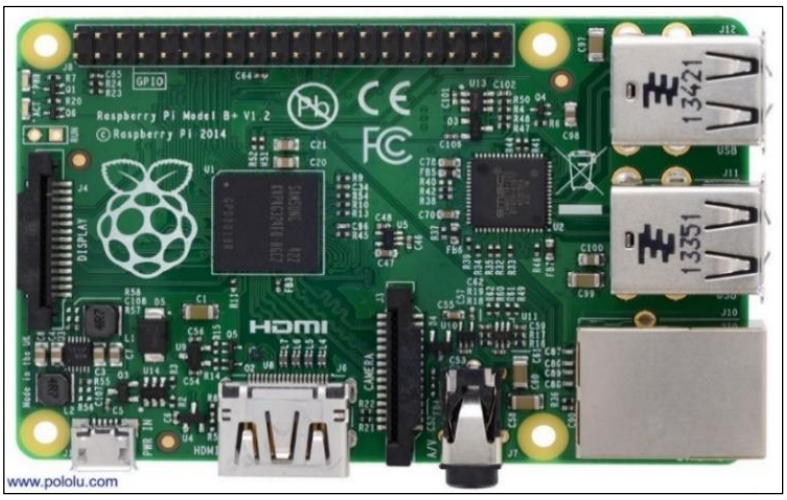

Figure 4: Raspberry Pi model B+.
Source: Authors, (2024).

III.3 ANALYSIS AND DESCRIPTION OF THE PHOTOVOLTAIC PARK CONNECTED TO THE GRID.

The park is located in the southwest area of the Faculty of Electrical Engineering of the "Marta Abreu" Central University of Las Villas, which injects energy into the network through a 315 V/34.5 kV central connection transformer.

It has 189 supporting structures, with 4x5 modules of 265 Wp, organized in 15 rows with a separation of 2.60 m, each row with 252 photovoltaic modules, the length of the rest structure is 3.97 m and the length of the tables in rows is 107 m, with an array width of 95 m, in addition, the photovoltaic modules are anchored to the metal structures with a plane of 19º with respect to the horizontal and facing pure South (azimuth 0º). It has a small automatic control room that houses the general protection and measurement cabinets, with basic facilities to support verification and maintenance tasks.

It has completed technological equipment:

• 3780 silicon (polycrystalline) photovoltaic modules, with a design of 21 modules in series and 3 branches in parallel to achieve the required voltage and current.

• Connections between modules using cables with multi-contact type connectors, guaranteeing quick installation with maximum reliability and durability of the connections.

• It has an independent power supply for plant service that ensures energy for the vitality of the inverters, the monitoring and physical protection system.

• It has a remote supervision system for communication, registration and data transmission, where two independent communication channels are used, as established by the Electrical Union regulations, in addition to external sensors to monitor additional meteorological variables.

The basic composition of the photovoltaic system, shown in figure 5, is given by the panel that generates direct current power through energy conversion. To stabilize the output voltage and reach the values required by the user, a DC-DC converter is used, which generally uses a boost converter so that the voltage generated in the cells is in the desired range, taking values up to ten times more than that generated by the photovoltaic cell.

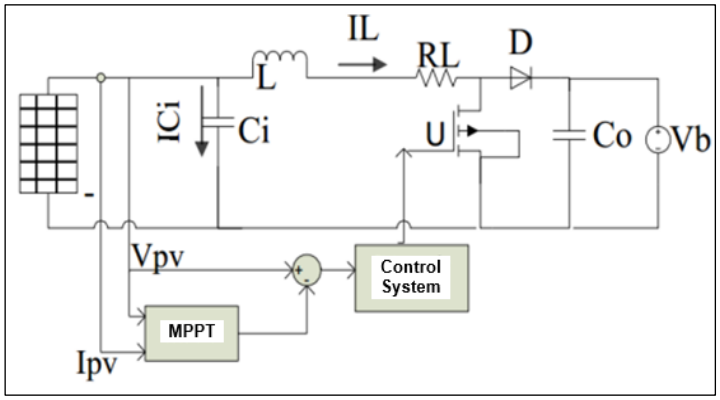

Figure 5: Composition of the photovoltaic system.
Source: Authors, (2024).

Photovoltaic systems connected directly to the electrical grid differ from those installed in isolation in that they do not have an energy accumulation bank or backup in the absence of solar radiation; These systems deliver directly to the network according to the standards and requirements of the electricity company (UNE) and their composition is broken down in figure 6.

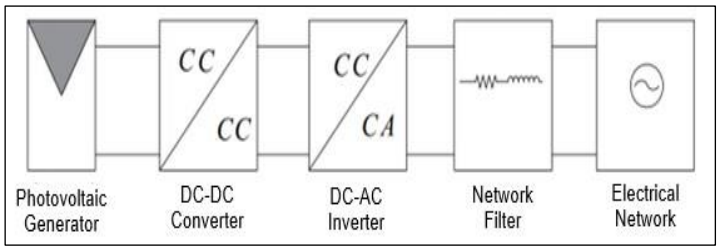

Figure 6: Photovoltaic system connected to the electrical grid.
Source: Authors, (2024).

The UCLV photovoltaic park is taken as an example:

Photovoltaic Generator: 265W Peak Hour Photovoltaic Solar Modules, Manufacturer Shanghai Aerospace Automobile Electromechanical Co.,Ltd. (HT-SAAE), model HT60 156P-265, with voltage at the maximum power point of 30.5 V, current at the maximum power point equal to 8.70 A, open circuit voltage 37.6 V, short circuit current at 9.28 A and efficiency approximately 16.3%.

Inverters: it has two Chinese-made inverters from 2015, SUNGROW SG500MX with: nominal input voltage 460-850V, nominal current 1220 A, operating temperature – 40…+65 °C and with an input at the maximum power point. The output values have a nominal power of 500 kW, maximum current of 1008 A and nominal voltage of 315V for three-phase connection and variable frequency 45-55 Hz and 55-65 Hz.

The performance of the photovoltaic solar park is monitored from a control booth where operators can supervise remotely through conventional communication systems (SCADA) [32].

III.4 MODELING OF THE PHOTOVOLTAIC PARK AT UCLV.

To simulate the behavior of a system similar to the Physical Twin of the photovoltaic park of the Universidad Central de las Villas, the mathematical software tool Simulink Matlab R2023b is used, developing a model that represents an installation connected to the grid. This model includes the following components: a photovoltaic solar panel, a DC-DC boost converter, the Perturbation and Observation (P&O) algorithm for maximum power point tracking (MPPT), the inverter which features voltage source control (VSC) and finally an output transformer to the electrical network.

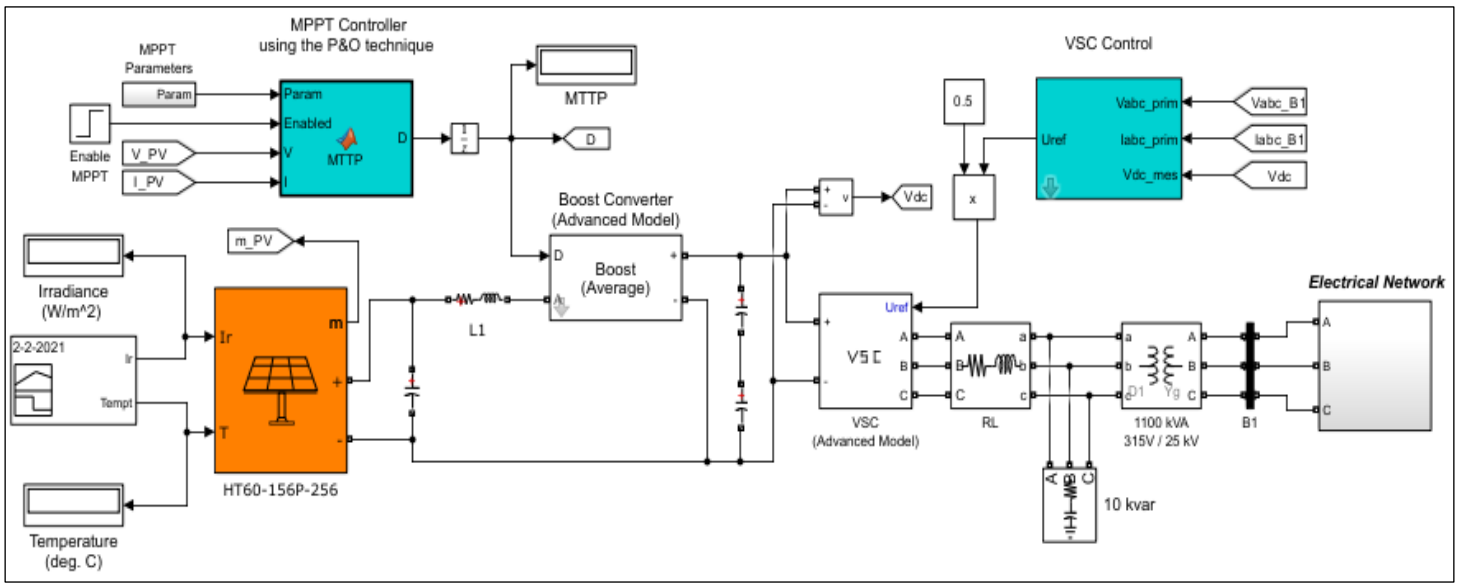

Figure 7: Digital Twin Model of the UCLV photovoltaic park.
Source: Authors, (2024).

Operation and description of the photovoltaic solar panel or PV array block.

The PV array block implements a series of photovoltaic modules. The array is made up of chains of modules connected in parallel, and each chain consists of modules connected in series. This block allows you to model preset PV modules from the National Renewable Energy Laboratory (NREL) Systems Advisor model (January 2014) under standard test conditions (STC) (irradiance=1000 W/m^2, temperature=25 °C), as well as the photovoltaic modules that you define. In this case, the photovoltaic module is defined as it is not pre-established, consisting of 180 modules connected in parallel, and each one consists of 21 modules connected in series.

After testing using constant temperature and irradiance inputs of 25ºC and 1000W/m^2 respectively, an error was discovered in the PV array block. This specific error only appeared when a fixed-step solver was applied and the "Break algebraic loop in internal model" option was enabled in the "Advanced" tab to generate C code from the model. The problem originated at a certain time, where the exponential used in the linearized equation of the photovoltaic panel diode reached an infinite value, resulting in the abrupt termination of the simulation.

Due to the error that occurred in the PV array block and that prevented its operation, the decision was made to replace said block with the electrical circuit that represents the photovoltaic solar panel, as shown in figure 3. In this way, the final model shown in figure 8 was obtained. This final model has the same elements as the main model, with the only difference that a subsystem is used to model the photovoltaic panel. However, it is important to highlight that in this new model it is not possible to use temperature as an input parameter, since the selected diode does not have a port for temperature.

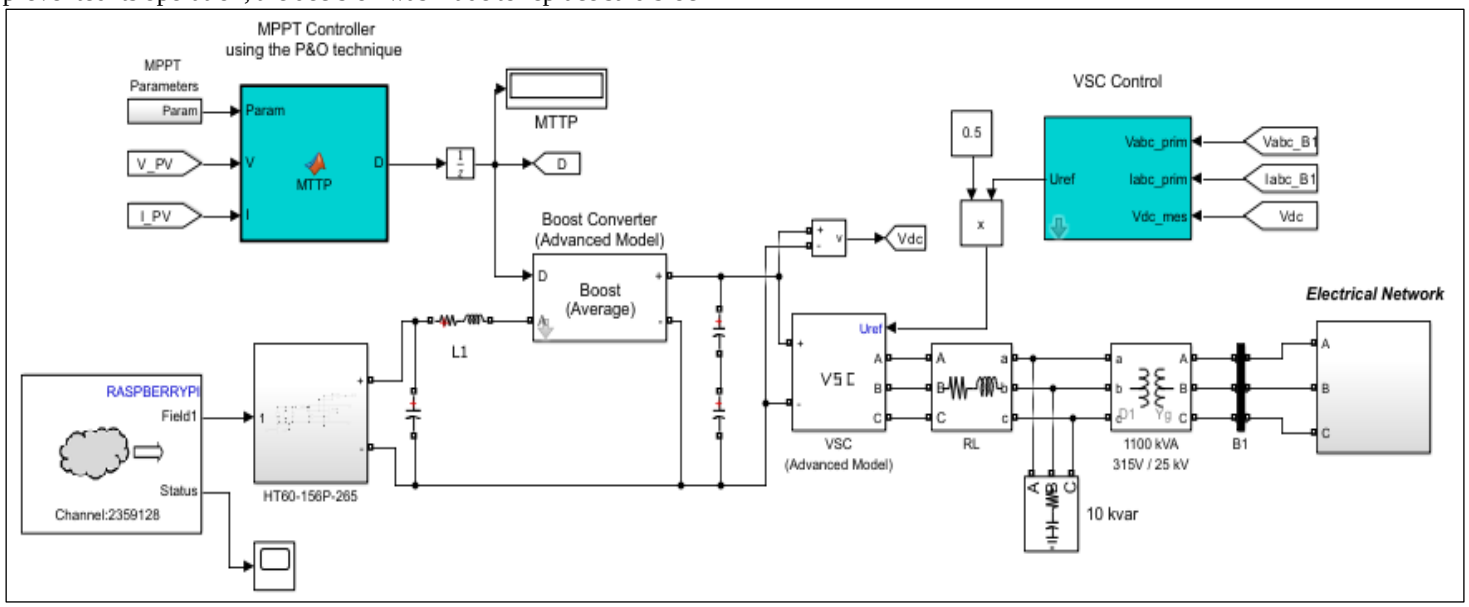

Figure 8: Digital Twin Model of the UCLV photovoltaic park with the electrical circuit subsystem of the photovoltaic panel.
Source: Authors, (2024).

Inside the photovoltaic panel subsystem there is the corresponding electrical circuit, which is represented in figure 9:

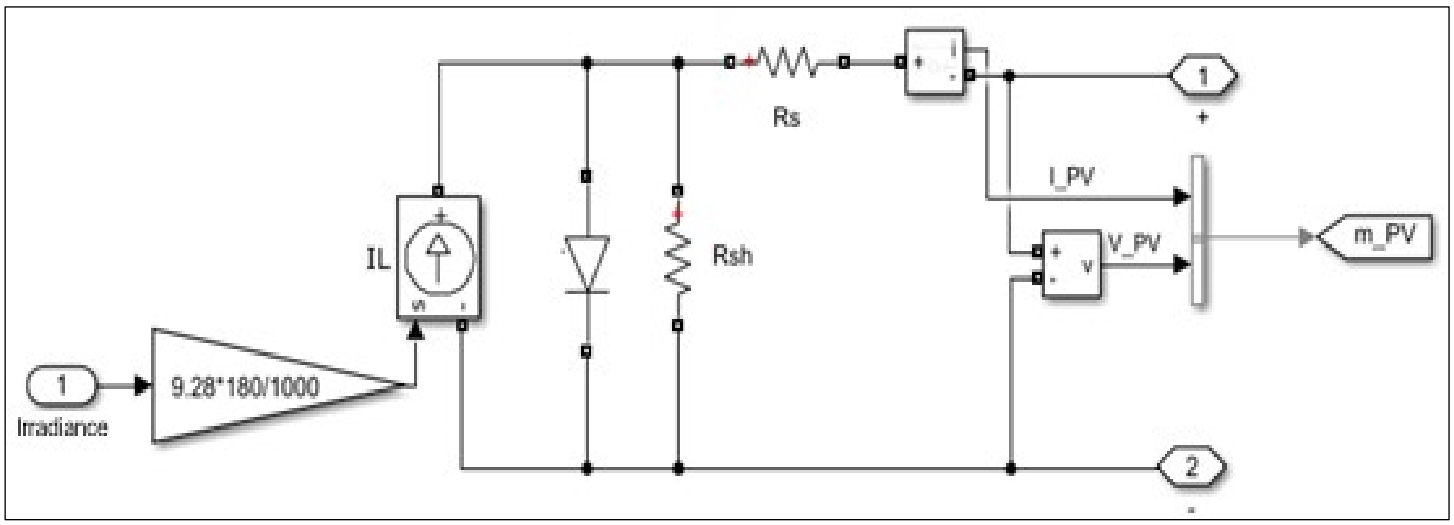

Figure 9: Electrical circuit of the photovoltaic panel.
Source: Authors, (2024).

Description of DC-DC Boost Converter and P&O algorithm for MPPT:

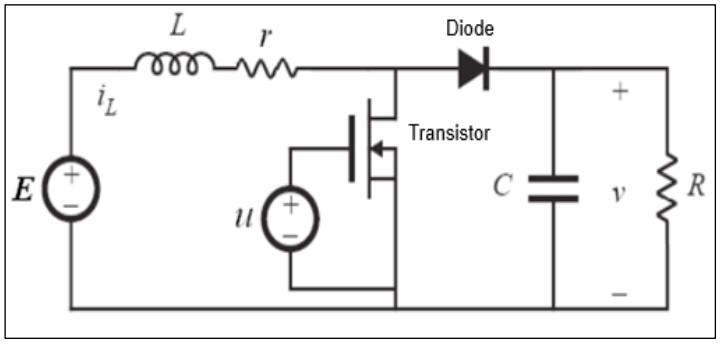

Figure 10: Boost converter with transistor and diode.
Source: Authors, (2024).

A Boost or DC-DC converter is used, being a voltage boosting circuit, which uses the characteristics of the inductor and the capacitor as energy storage elements to raise the current coming from the power supply and use it to inject it into the capacitor. Thus, producing higher voltage levels at the load than at the source [33].

The maximum power point is tracked to maintain optimal system charging based on the solar panel inputs. The implementation of the MPPT is carried out using the perturbation and observation (P&O) algorithm. This algorithm consists of observing the voltage variation as a function of power, so that the increase in voltage is compared with the increase in power. If both increments are of the same sign, it means that the operating voltage has to increase to reach the maximum power point (MPP) and if they are of different sign the operating voltage has to decrease. With this algorithm, the duty cycle of the boost converter is adjusted, achieving the desired setting.

Voltage Source Controlled (VSC) Inverter Operation:

A power inverter is an electronic power converter, its main function is to facilitate the exchange of energy between two or more subsystems and this is achieved by transforming continuous signals (DC) to alternating signals (AC). The task can be performed through a wide variety of configurations in which we find (electronic) power switches, passive components and a control system that also has the protection function. The link between the control system and the power switches is through switching signals. These switching signals act on the power switches, controlling their switching (ON and OFF). By properly switching these power switches we achieve proper transfer of power from the DC side to the AC side. A type of average model voltage source converter is used to represent power electronic switches. Unlike other power electronic devices, this model uses reference signals (Uref) that represent the average voltages generated at the ABC terminals of the bridge. This model does not represent harmonics. It can be used with longer sampling times while preserving average voltage dynamics [34].

The VSC inverter is a device that offers precise control over the generated alternating current output waveform. It provides high power quality, regulation capability, reactive power injection, fast response and design flexibility. These features make the VSC inverter a popular choice in renewable energy systems and electrical transmission applications.

Description of the mains connection transformer:

The output transformer has two main functions: voltage matching, it allows the output voltage of the converter to be adjusted to match the mains voltage, and impedance matching, it is used to match the output impedance of the converter to the impedance of the electrical network. This ensures that power transfer between the converter and grid is efficient and minimizes wave reflections. It is composed of two or more coils of wire wound around a laminated iron core. The primary coil is connected to the voltage source converter and the secondary coil is connected to the mains. The turns ratio between the coils determines the voltage transformation ratio. In addition to the voltage and impedance matching function, it also provides galvanic isolation between the converter and the mains. This means there is complete electrical separation between the two, ensuring safety and preventing the transfer of unwanted currents [35].

The transformer present in the UCLV has a power capacity of 1100 kVA, being the maximum, it can deliver to the connected load. The transformation ratio is expressed as 315 V/34.5 kV. This means that the primary (input) voltage is 315 volts (V) and the secondary (output) voltage is 34.5 kilovolts (kV). Transformers are passive devices and do not directly modify power. Its main function is to adapt voltage and current levels for the efficient transmission of electrical energy between different systems or loads.

IV. CONFORMATION OF THE DIGITAL TWIN OF THE UCLV PHOTOVOLTAIC FIELD.

IV.1 INTEGRATION, COMMUNICATION AND IMPLEMENTATION OF THE DIGITAL TWIN.

Once the Digital Twin model has been obtained and its implementation on the Raspberry Pi, it is necessary to establish bidirectional communication between the Digital Twin and the real plant. This involves finding suitable connection methods between the Raspberry Pi and the physical system. The real plant must send the data obtained from its sensors to the Digital Twin to ensure that both models have the same input parameters. Additionally, both models must be able to exchange output data for later comparison. In this sense, two viable options are presented for a secure and orderly exchange of data between both entities. One option is by using Sockets, it is defined by two IP addresses (one for the local computer and one for the remote computer), a transport protocol and two port numbers that identify the programs involved. Another option is to use the cloud as a platform for data exchange. In this case, the ThingSpeak tool can be used to establish the connection. The actual plant collects input data from IoT sensors and stores it in specific ThingSpeak fields. The Digital Twin accesses this data to use as input parameters in its model. Likewise, both the real plant and the Digital Twin send the output data to separate fields in ThingSpeak. It is chosen to save the information obtained from the model in a text file (CSV). This choice facilitates access to the data from Matlab and allows a simple comparison with the results obtained from the real plant.

The Raspberry Pi is used to implement the Digital Twin due to its ability to meet the necessary hardware requirements. To do this, two support packages are installed, one for Matlab ("MATLAB Support Package for Raspberry Pi Hardware") and another for Simulink ("Simulink Support Package for Raspberry Pi Hardware") on the Raspberry Pi. On the other hand, the development of the solar plant model is carried out in two programming environments: Simulink and PV_LIB.

In each of these environments, different methods are used to obtain the virtual model. In Simulink, it is built using a block diagram, which can be converted to C code thanks to one of the applications of these tools. On the other hand, in PV_LIB, the virtual model is developed by using the specific functions provided by this Toolbox.

The model represented in figure 8 illustrates the Digital Twin developed in Simulink. The limitation of this model is that it has not been possible to incorporate the effect of temperature in the electrical circuit of the photovoltaic panel (Figure 9). This is

because the diode used does not allow the temperature port to be displayed, so we will only work with irradiance as an input parameter. As a result, this model does not realistically represent the UCLV photovoltaic park, since temperature is a crucial factor that affects the output power of the photovoltaic panel. However, the advantage of this model is that it uses the same components as the physical model, making it an accurate representation of the solar PV plant in that regard.

To transfer the models developed in Simulink to the Raspberry Pi, there are two alternatives to generate this code. The first is to use the Simulink Embedder Coder Toolbox, through the Matlab Coder package. The C code is generated, the "main" is modified to save the variables in a text file (.txt) and the folder with the code is sent to the Raspberry Pi, being executed in the terminal and obtaining the variables from Matlab with location on the Raspberry Pi using communication established by SSH. The second alternative, which is the one used, involves generating the code directly on the Raspberry Pi, without the need to make subsequent modifications. This allows for a more direct and efficient transfer of models from Simulink to the Raspberry Pi.

The model built with PV_LIB is made up of a photovoltaic solar system, since these are the elements that this tool models. The same photovoltaic panel is used with the same characteristics as that used in the Simulink model. This allows a direct comparison of the results obtained from both models, since it is based on a consistent basis. The input values are obtained, defining the cell temperature at 25 °C. The .m file is then converted into a function that can be sent to the hardware board in Simulink, with the PV_LIB model implemented.

The main advantage of this approach is that it allows the effects of irradiance and temperature at the input of the photovoltaic panel to be easily modeled, unlike the Simulink model where it was not possible to include temperature as an input variable. However, a limitation of this method is that additional components such as converters, transformer or tracking algorithms cannot be added to obtain a complete model of a solar PV plant, since the corresponding functions are not defined. Another drawback is that it is not possible to establish a direct connection to the Raspberry Pi because Matlab code generation does not support PV_LIB functions. As a result, the behavior of this model can only be visualized in Matlab and it does not faithfully represent the complete operation of the photovoltaic park, but only the solar panel.

IV.2 RESULTS OBTAINED FROM THE DIGITAL TWIN WITH THE REAL PLANT.

A visit is made to the UCLV photovoltaic park, where the input (irradiation and temperature) and output (active power) data of the Gemelo Real (photovoltaic system) were provided. Data from the photovoltaic park system connected to the grid was obtained, in a 12-hour sample, on February 2, 2021.

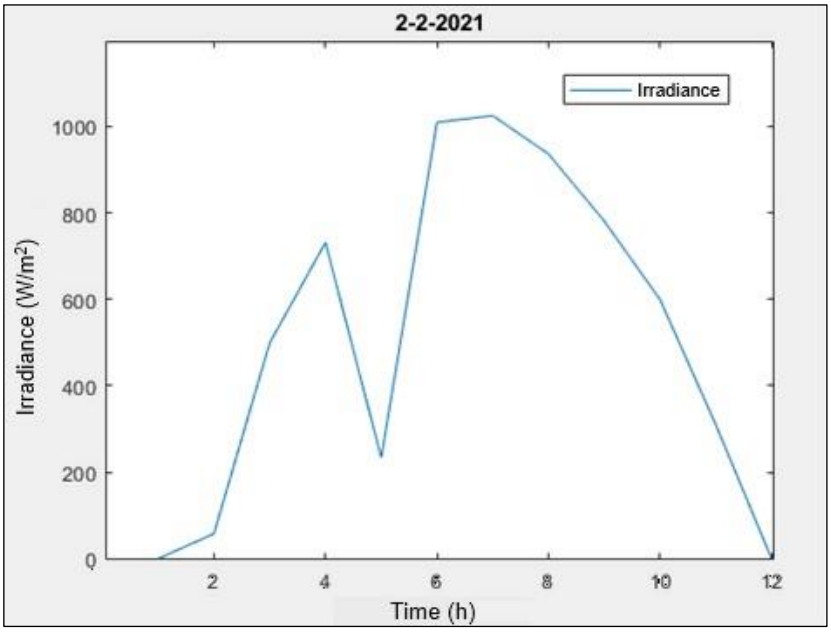

Figure 11: Irradiance input parameter.
Source: Authors, (2024).

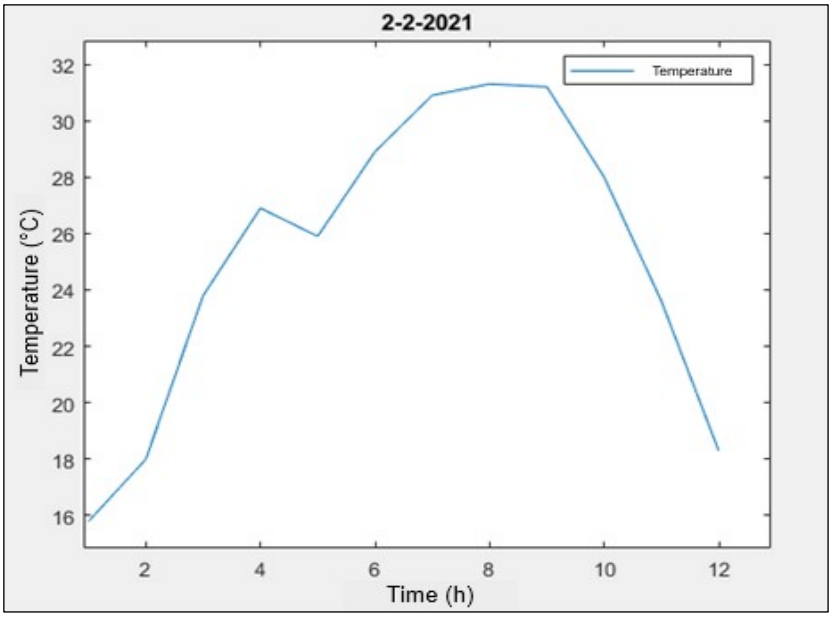

Figure 12: Temperature input parameter.
Source: Authors, (2024).

Digital Twin Model of the UCLV photovoltaic park.

The model used in the faithful representation of the UCLV photovoltaic park is used in the comparison between Simulink and the Real Twin, figure 13. The purpose of this model is to validate the operation only in the Simulink development environment, because it has the PV array block, which makes its implementation on the Raspberry Pi impossible.

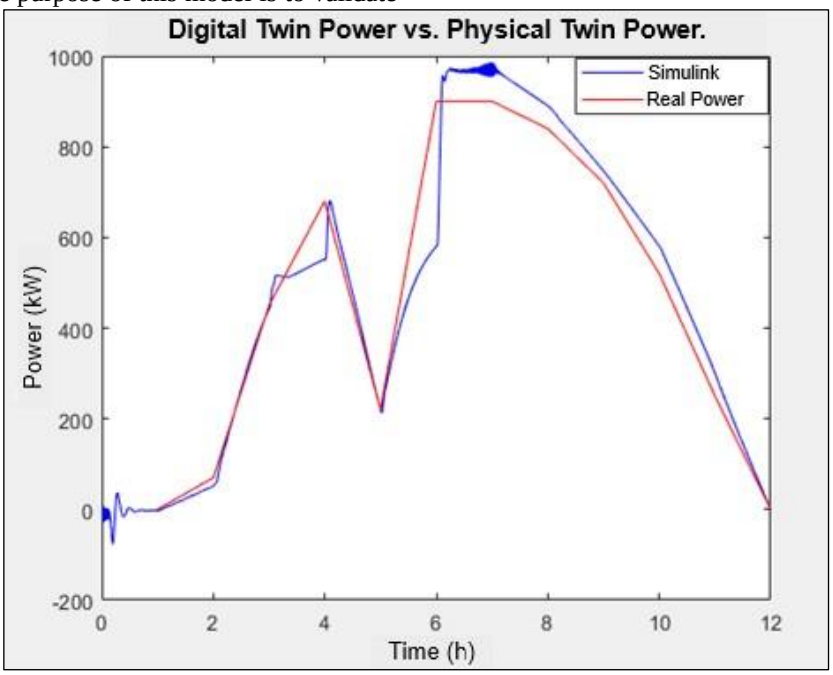

Figure 13: Comparison of powers between the outputs of the models.
Source: Authors, (2024).

Performing a statistical analysis, the square root of the root mean square error (RMSE) is calculated to evaluate the accuracy of the forecast model, which provides a quantitative measure of how close the predicted values are to the actual values, resulting in 51.04 kW (4.64 % precision error).

Model of the electrical circuit of the photovoltaic panel present at the UCLV.

In this comparative study between PV_LIB, Simulink and Raspberry Pi, the model that represents an electrical circuit of a solar panel is used (figure 9). The objective is to validate the operation of the developed circuit, and all models are configured with the same parameters and the same irradiance input. Although PV_LIB allows temperature to be entered as an additional input, the Simulink model does not include this option and only works with irradiance.

In Simulink, a load is added to the circuit by including a resistor whose value corresponds to the relationship between the voltage at the maximum power point and the current at the maximum power point. This guarantees optimal loading conditions for the model to reach the maximum power point (MPPT). Since

these values of the maximum power point correspond to an irradiance of 1000 W/m^2.

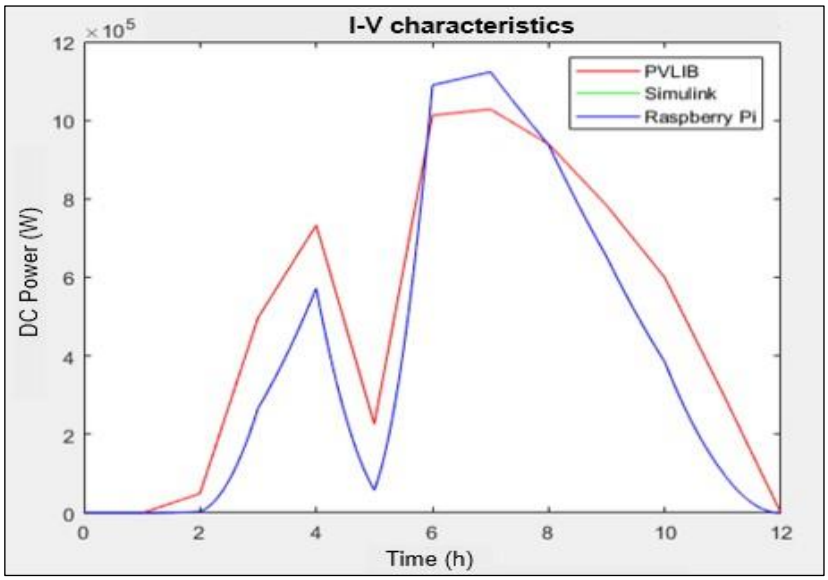

Figure 14: Pmp output signal comparison.
Source: Authors, (2024).

It can be seen that the outputs generated by Simulink and the Raspberry Pi in the graph are completely the same. This is because the sampling period of the hardware board is smaller than that of Simulink, therefore the Digital Twin is running in real time in both cases, which guarantees precise synchronization between the results obtained.

In terms of the results obtained, it is expected to reach specific values at the maximum power point, such as Vmp = 640.5 V, Imp = 1566 A and Pmp = 1.003 MW. These values exactly match the outputs of the model implemented in PV_LIB, confirming that the model developed in this tool works correctly. However, Simulink returns higher values (Vmp = 559.1 V, Imp = 1960 A, Pmp = 1.095 MW). This is because, although Simulink represents circuit losses using series and parallel resistors, there are differences in the parameters compared to the PV_LIB model. The reason for these discrepancies is that the PV_LIB model is more precise, since it takes into account all the variables and nonlinearities of the solar panel.

Regarding the data achieved by the sample values, the result is an RMSE value of 136.03 kW precision of the Simulink and Raspberry Pi model with respect to PV_LIB.

Complete model of the UCLV photovoltaic park.

In order to analyze the effects of a complete solar photovoltaic installation, a comparative study is carried out using the model presented in Figure 8. Although it is not possible to define all the components using the functions provided by PV_LIB, this model can be used for comparison. with Simulink and its implementation on the Raspberry Pi, assuming that the solar panel is operating at the maximum power point. Since this model is more complex than the one presented above, it is necessary to evaluate whether the board is capable of running the Digital Twin in real time.

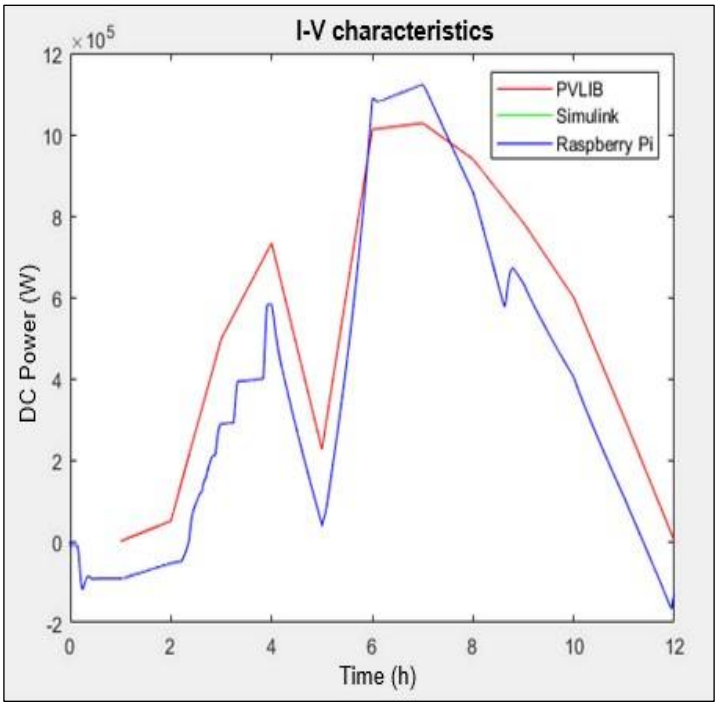

Figure 15: Comparison of Pmp output in the full model.
Source: Authors, (2024).

In relation to the data obtained in the sample, an accuracy of 146.46 kW has been obtained from the Simulink and Raspberry Pi model compared to PV_LIB.

Figure 16 shows the comparison between the power generated by the photovoltaic solar installation and the power of the Digital Twin model, the PV array block has been replaced by the photovoltaic panel circuit and the irradiance input variable has been used to simulate solar radiation conditions. This comparison allows us to evaluate how the Digital Twin behaves in terms of power generation in relation to the Physical Twin.

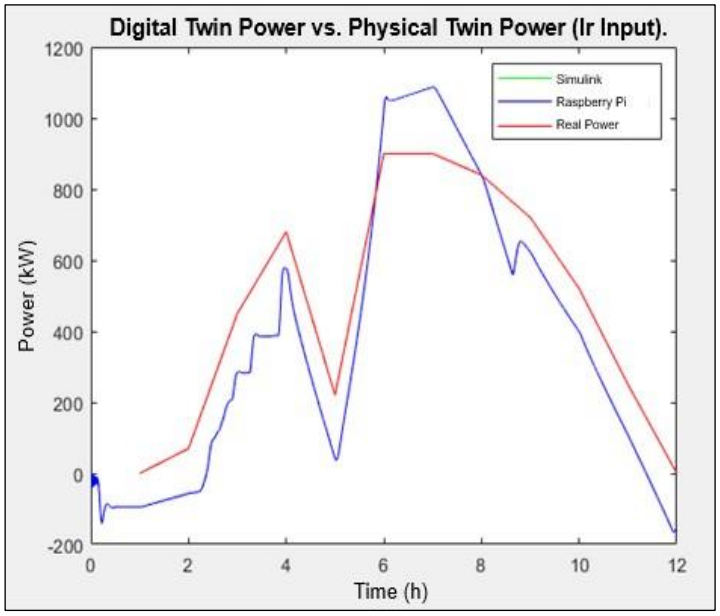

Figure 16: Comparison of output powers.
Source: Authors, (2024).

Statistical analysis reveals a root mean square error value of 134.02 kW (12.18%), which evaluates the accuracy of the forecast model by measuring the proximity of the predicted values to the actual values.

V. CONCLUSIONS

A Digital Twin of the photovoltaic park installed at the UCLV has been created, using the Matlab programming environment together with the Simulink and PV_LIB tools, executing the C code on a Raspberry Pi model B+, which has allowed the system to be implemented and controlled in time. real. During the implementation of the Digital Twin, challenges have been faced due to the novel nature of this technology and its current limitations. Obtaining significant results:

A comparison of the ideal model was carried out between the power generated in Simulink and the real power of the UCLV photovoltaic park, obtaining an RMSE of 51.04 kW, with a precision error of 4.64% in the power estimation.

The full model, in terms of power generation of the Digital Twin in relation to the Physical Twin the RMSE value is 134.02 kW, this implies a precision error discrepancy of 12.18% in the power estimation.

VI. AUTHOR'S CONTRIBUTION

Conceptualization: Luis Gabriel Fong Mollineda and José Rafael Abreu García.
Methodology: Luis Gabriel Fong Mollineda and José Rafael Abreu García.
Investigation: Luis Gabriel Fong Mollineda and José Rafael Abreu García.
Discussion of results: Luis Gabriel Fong Mollineda and José Rafael Abreu García.
Writing – Original Draft: Luis Gabriel Fong Mollineda and José Rafael Abreu García.
Writing – Review and Editing: Luis Gabriel Fong Mollineda and José Rafael Abreu García.
Resources: Luis Gabriel Fong Mollineda and José Rafael Abreu García.
Supervision: Luis Gabriel Fong Mollineda and José Rafael Abreu García.
Approval of the final text: Luis Gabriel Fong Mollineda and José Rafael Abreu García.

VIII. REFERENCES

[1] Z. Song *et al.*, "Digital Twins for the Future Power System: An Overview and a Future Perspective," *Sustainability 2023, Vol. 15, Page 5259*, vol. 15, no. 6, p. 5259, Mar. 2023, doi: 10.3390/SU15065259.

[2] I. Tecnológico, S. Jubones, M. Lourdes, C. Linares-Vizcarra, E. T. Montero-Zuñiga, and J. Luna-Nemecio, "Ecología, energías renovables y sustentabilidad socioformativa," *Sociedad & Tecnología*, vol. 6, no. 2, pp. 261–274, May 2023, doi: 10.51247/ST.V6I2.371.

[3] C. del Bosque Peón, "Los gemelos digitales en la industria 4.0," 2019, Accessed: Feb. 28, 2024. [Online]. Available: http://uvadoc.uva.es/handle/10324/40037

[4] K. Arafet Cruz, "Gemelo Digital en Parques Solares: enfoque mediante series temporales y aprendizaje profundo," Nov. 2020, Accessed: Feb. 28, 2024. [Online]. Available: https://repositori.uji.es/xmlui/handle/10234/193565

[5] "Gemelo digital de centrales solares fotovoltaicas: prueba de concepto Girasol | Artículos y entrevistas." Accessed: Jun. 29, 2023. [Online]. Available: https://energetica21.com/articulos-y-entrevistas-online-ver/gemelo-digital-de-centrales-solares-fotovoltaicas-prueba-de-concepto-girasol

[6] W. D. Chicaiza, J. Gómez, A. J. Sánchez, and J. M. Escaño, "El Gemelo Digital y su aplicación en la Automática," *Revista Iberoamericana de Automática e Informática industrial*, Feb. 2023, doi: 10.4995/RIAI.2024.20175.

[7] A. A. SALVADOR-NAVARRO, "Modelado de un gemelo digital para Internet de las Cosas," Oct. 2023, Accessed: Feb. 28, 2024. [Online]. Available: http://crea.ujaen.es/jspui/handle/10953.1/20475

[8] "Gemelos digitales: agregando inteligencia al mundo real - Capgemini España." Accessed: Jun. 01, 2023. [Online]. Available: https://www.capgemini.com/us-en/insights/research-library/digital-twins/#

[9] A. Bosch Serra, "Simulación de componentes de un vehículo eléctrico mediante gemelo digital," Nov. 2022, Accessed: Feb. 29, 2024. [Online]. Available: https://riunet.upv.es:443/handle/10251/190137

[10] M. V. Chiquito, M. V. Chiquito, J. C. G. Plua, M. B. Chong, and C. B. Chong, "Gemelos digitales y su evolución en la industria," *RECIMUNDO*, vol. 4, no. 4, pp. 300–308, Nov. 2020, doi: 10.26820/recimundo/4.(4).noviembre.2020.300-308.

[11] L. Massel, N. Shchukin, and A. Cybikov, "Digital twin development of a solar power plant," *E3S Web of Conferences*, vol. 289, p. 03002, Jul. 2021, doi: 10.1051/E3SCONF/202128903002.

[12] D. S. Moreno Esparza, A. J. Escárraga González, M. en A. de E.-M.-V. 63320946, and M. en A. de E.-M.-V. 1015397124, "Análisis de la Factibilidad de la Implementación de Sistemas de Energía Fotovoltaica en Residencias Rurales de Chocontá-Cundinamarca," 2024, Accessed: Feb. 28, 2024. [Online]. Available: https://repository.universidadean.edu.co/handle/10882/13208

[13] A. SALAZAR-PERALTA, P.-S. Alfredo, and U. PICHARDO, "La energía solar, una alternativa para la generación de energía renovable," *Revista de Investigación y Desarrollo*, vol. 2, no. 5, pp. 11–20, 2016.

[14] A. Beléndez, "Einstein 1905: De los «cuantos de energía» a los «cuantos de luz»," Nov. 2015, Accessed: Feb. 29, 2024. [Online]. Available: http://rua.ua.es/dspace/handle/10045/95405

[15] V. Ossa Arango, "Ensamble y caracterización de un panel solar fotovoltáico." Pereira: Universidad Tecnológica de Pereira, 2017. Accessed: Mar. 01, 2024. [Online]. Available: https://repositorio.utp.edu.co/handle/11059/7616

[16] H.-L. Tsai, T. Ci-Siang, and S. Yi-Jie, "Development of generalized photovoltaic model using MATLAB/SIMULINK," *Lecture Notes in Engineering and Computer Science*, vol. 2173, Mar. 2008.

[17] E. Granda-Gutiérrez, O. Orta, J. C. Díaz-Guillén, M. Jiménez, M. Osorio, and M. González Albarrán, "MODELADO Y SIMULACIÓN DE CELDAS Y PANELES SOLARES," Mar. 2013. doi: 10.13140/2.1.4192.8968.

[18] W. De Soto, S. A. Klein, and W. A. Beckman, "Improvement and validation of a model for photovoltaic array performance," *Solar Energy*, vol. 80, no. 1, pp. 78–88, Jan. 2006, doi: 10.1016/J.SOLENER.2005.06.010.

[19] X. H. Nguyen and M. P. Nguyen, "Mathematical modeling of photovoltaic cell/module/arrays with tags in Matlab/Simulink," *Environmental Systems Research 2015 4:1*, vol. 4, no. 1, pp. 1–13, Dec. 2015, doi: 10.1186/S40068-015-0047-9.

[20] "Item 1004/2338 | Repositorio CIMAV." Accessed: Sep. 04, 2023. [Online]. Available: https://cimav.repositorioinstitucional.mx/jspui/handle/1004/2338

[21] T. Ahmad, S. Sobhan, Md. F. Nayan, T. Ahmad, S. Sobhan, and Md. F. Nayan, "Comparative Analysis between Single Diode and Double Diode Model of PV Cell: Concentrate Different Parameters Effect on Its Efficiency," *Journal of Power and Energy Engineering*, vol. 4, no. 3, pp. 31–46, Mar. 2016, doi: 10.4236/JPEE.2016.43004.

[22] A. Krenzinger and C. W. Massen Prieb, "Clasificación y selección de módulos fotovoltaicos para una central conectada a la red," *Avances en Energías Renovables y Medio Ambiente*, vol. 9, 2005, Accessed: Feb. 28, 2024. [Online]. Available: http://sedici.unlp.edu.ar/handle/10915/82225

[23] "Partes de un panel solar, estructura y componentes." Accessed: Sep. 10, 2023. [Online]. Available: https://solar-energia.net/energia-solar-fotovoltaica/elementos/panel-fotovoltaico/estructura-de-un-panel-fotovoltaico

[24] M. A. Abella, "Sistemas fotovoltaicos," *SAPT Publicaciones Técnicas, SL*, 2005.

[25] H. Moore, V. C. Olguín, and R. M. Nuño, *MATLAB para ingenieros*, no. 620.0013 M66 2007. Pearson Educación, 2007.

[26] L. Matlab, "MATLAB & Simulink." Retrieved September, 2021.

[27] J. S. Stein, "The photovoltaic Performance Modeling Collaborative (PVPMC)," in *2012 38th IEEE Photovoltaic Specialists Conference*, 2012, pp. 3048–3052. doi: 10.1109/PVSC.2012.6318225.

[28] M. A. G. Maureira, D. Oldenhof, and L. Teernstra, "ThingSpeak–an API and Web Service for the Internet of Things," *World Wide Web*, vol. 25, pp. 1–4, 2011.

[29] T.-H. Lee, K.-H. Lee, G.-T. Ahn, and M.-J. Lee, "Sharing Display Based on VNC," in *Proceedings of the Korean Information Science Society Conference*, Korean Institute of Information Scientists and Engineers, 2008, pp. 241–244.

[30] M. Richardson and S. Wallace, *Getting started with raspberry PI*. " O'Reilly Media, Inc.," 2012.

[31] "Pololu - Raspberry Pi Model B+." Accessed: Nov. 30, 2023. [Online]. Available: https://www.pololu.com/product/2752

[32] J. Borges, J. García, and A. Martínez, "Comparación de algoritmos MPPT aplicados a sistemas fotovoltaicos," 2018.

[33] F. F. Valderrama Gutiérrez, H. Moreno C, and H. M. Vega, "Análisis, simulación y control de un convertidor de potencia DC- DC tipo boost," *Ingenium, ISSN 0124-7492, Vol. 12, Nº. 24, 2011 (Ejemplar dedicado a: INGENIUM), págs. 44-55*, vol. 12, no. 24, pp. 44–55, 2011, Accessed: Mar. 01, 2024. [Online]. Available: https://dialnet.unirioja.es/servlet/articulo?codigo=5038442&info=resumen&idioma=SPA

[34] J. C. Jorge and C. L. Eloy, "Control de un inversor fotovoltaico conectado a la red eléctrica trifásica," 2011.

[35] L. D. Caiza Betancourt, "Análisis dinámico para el diagnóstico de transformadores de potencia basada en su condición," 2024, Accessed: Mar. 01, 2024. [Online]. Available: http://dspace.ups.edu.ec/handle/123456789/26770